Available online at www.sciencedirect.com

ScienceDirect

Advances in Space Research xxx (xxxx) xxx

ADVANCES IN SPACE RESEARCH
(a COSPAR publication)

www.elsevier.com/locate/asr

Reckoning ionospheric scintillation S4 from ROTI over Indian region

Chandan Kapil [a], Gopi K Seemala [a,*], Dadaso J Shetti [b], Rajat Acharya [c]

[a] Indian Institute of Geomagnetism, Navi Mumbai, India
[b] Smt. Kasturbai Walchand College, Sangli, India
[c] Space Application Center, ISRO, Ahmedabad, India

Received 3 May 2021; received in revised form 6 October 2021; accepted 13 October 2021

Abstract

Ionospheric irregularities cause fluctuations (scintillations) in received satellite signal strength, degrading communication and navigation signals. The scintillation strength depends on the scale sizes of the irregularities and the frequency of the radio signal. The parameter S4 index describes the scintillation strength derived from the amplitude of high rate received signal sampled at 50 Hz, usually from special GNSS receivers. Most GNSS receivers have a lower data sampling rate, so an alternate parameter, Rate of Change of TEC Index (ROTI), is derived from the total electron content (TEC) sampled at 30 s. Here, the correlation between ROTI and S4 is performed for the Indian ionospheric region, with different elevation mask angles and ROTI calculated over different averaging intervals. An estimate of the S4 value from ROTI is unreliable even though the correlation between them is better than 0.6. Different elevation mask angles and ROTI with varying averaging intervals do not significantly affect the correlation between S4 and ROTI. Further, the correlation and occurrence percentages of S4 corresponding to ROTI are analyzed. An 80% confidence range is obtained to correlate the observed ROTI with the corresponding S4 index. These probability estimates of S4 values derived from ROTI values also vary with latitude. This relation between ROTI and S4 will be beneficial in using standard GNSS receivers for the studies of ionospheric scintillations.

Keywords: Ionospheric irregularities; ROTI; Total electron content; Correlation between ROTI & S4

1. Introduction:

Fluctuations in the received phase or amplitude of radio signals traversing the ionosphere are known as scintillations (Yeh & Liu, 1982). Intense signal fluctuations may cause Global Navigation Satellite System (GNSS)/ Global Position System (GPS) receivers to stop tracking or locking on to the signals from satellites. The latter phenomenon is known as "loss of lock." The reduction in the number of visible satellites may decrease the position accuracy, cause fluctuations in the estimated position or in many cases, may even cause navigation failure. Also, these fluctuations are measured to study ionospheric irregularities. These scintillations are caused by the diffraction of radio wave signals passing through the moving (small or medium-scale) electron density irregularities in the ionosphere (Kintner et al., 2007). The signals that pass through the ionospheric irregularities experience changes in the refractive index. A radio wave signal that enters the irregular medium with a uniform phase will experience phase changes due to the diffraction phenomenon. Received signals may combine either constructively or destructively to increase or decrease the wave amplitude, resulting in amplitude fluctuations (Kintner et al., 2007; Yeh & Liu, 1982). The scintillation occurrence is highly dependent on season, solar activity and geographical locations. Other factors can affect these irregularities, such as space weather conditions and induced ionospheric electric and magnetic fields. Ionospheric scintillations observed through GPS receivers at the

* Corresponding author.
E-mail address: gopi.seemala@iigm.res.in (G.K Seemala).

https://doi.org/10.1016/j.asr.2021.10.026
0273-1177/

Please cite this article as: C. Kapil, G. K. Seemala, D. J. Shetti et al., Reckoning ionospheric scintillation S4 from ROTI over Indian region, Advances in Space Research, https://doi.org/10.1016/j.asr.2021.10.026

L1 frequency (1.575 GHz) are called L-band scintillations, and hereinafter, we refer to them as scintillations.

Depletions in ionospheric plasma density in equatorial and low latitude regions are referred to as equatorial plasma bubbles and are generated through Rayleigh-Taylor (RT) instability mechanism (Fejer, 1997). In post-sunset hours, the ionization density and the dynamo action of the electric field in the E-region of the ionosphere decrease, and a dynamo-electric field develops in the F-region. The polarization charges set up by the longitudinal conductivity gradients at the day-night terminator enhance the eastward electric field for about an hour after sunset. This phenomenon is known as Pre-Reversal Enhancement (PRE) (Abadi et al., 2015). As ionization density decreases in the E-region after post-sunset hours, a steep vertical plasma density gradient forms in the bottom side F-region, which is opposite to the gravity vector (downwards). These conditions are conducive for Rayleigh-Taylor (RT) instability, allowing plasma density irregularities to form (Kelley, 1985; Huang & Kelley, 1996; Hysell, 2000). As they rise into the region above the peak of the F-layer, these irregularities can grow into large plasma depletions, generally known as Equatorial Plasma Bubbles (EPBs). The steep density gradients at the edges of the bubbles help generate smaller-scale irregularities responsible for the scintillations in L-band frequencies (Otsuka et al., 2009). Equatorial plasma bubbles can be detected as diffused echoes in ionograms, plumes in VHF radar maps, intensity bite-outs in night time OI 630 nm airglow intensity, electron density depletions in in-situ satellite measurements, and scintillations in VHF/L- band satellite beacon signals (Basu et al., 1978; Farley et al., 1970; Kelley, 1989; McClure et al., 1977; Ossakow, 1981; Rama Rao et al., 2006a).

With the onset of an era of navigation satellites, scintillations were investigated at higher frequencies, including those used by the GPS satellites, L-band (1.2 to 1.5 GHz). In a satellite-based navigation system, radio signals are adversely affected by ionospheric post-sun-set scintillations. Ionospheric scintillations thus draw interest to study their impact on radio signals. The intensity of ionospheric scintillations is indicated by two indices (1) amplitude scintillation index S4 and (2) Rate of Change of TEC Index (ROTI). The total electron content (TEC) is defined as the integral of electron density along the satellite-receiver path (Klobuchar et al., 1977). TEC is measured in electrons per square meter or TEC units (TECU). The 1 TECU is equal to 10^{16} electrons/m^2 (or el/m^2).

A special GNSS receiver known as an Ionospheric Scintillation Monitor (ISM), with signal amplitude observations at a sampling rate of 50 Hz or more is required to measure the S4 index (Yang & Liu, 2016a). Most often, standard GNSS receivers, because of their low data sampling cadence, i.e., 1 to 30 s, are technically unable to measure S4, which corresponds to irregularities of Fresnel scale size (Olwendo et al., 2018). Fresnel scale size is defined as $d_f = \sqrt{2\lambda z}$, where λ is free-space wavelength of the radio signal and z is the altitude. Now, for the GPS L1 wavelength of 0.19 m and at 350 km altitude irregularities, the Fresnel scale is $d_{f\,=}$ 360 m, also the timescale of GPS scintillation is 4 s as a consequence of equatorial irregularities with drift velocity of 100 m/s (Beach and Kintner, 1999; Jacobsen, 2014). At present several GNSS networks have been deployed throughout the world. Pi et al. (1997) suggested an index, known as ROTI to observe scintillations from low sampling data. ROTI is the standard deviation of the rate of change of TEC over a period of 5 min (Tiwari et al., 2013). In 2006, Ma and Maruyama stated that generally, ROTI greater than 0.5 TECU/min indicates the presence of ionospheric irregularities with scale sizes of a few kilometers. The Amplitude scintillation index S4 is defined as the normalized variance of the intensity of the signal. Basu et al., (1999) compared amplitude scintillation measurements of GPS-L1 frequency (1.575 GHz) signals with fluctuations of the TEC. They suggested that ROTI can be used as a proxy in place of S4, indicating the presence of small-scale ionospheric irregularities, especially in the equatorial region. They also suggested that the ratio of ROTI/S4 can vary between 2 and 10 and indicated that the variation of ROTI to S4 ratio is dependent on the geographical location. Several studies have been done by detecting ROTI and S4 simultaneously from the co-located instruments (Krankowski et al., 2006; Basu et al., 1999).

The results indicate that large normalized ROTI with small S4 and similarly large S4 with very small ROTI can be found, showing that ionospheric scintillations are not directly related to ROTI (Yang & Liu, 2016b). In many studies, it is found that during an intense scintillation event, a corresponding ROTI exists of proportional strength with S4. However, there is no definite relation between ROTI and S4, as many other factors cause scintillations apart from ionospheric irregularities such as multipath, tropospheric scatter, etc. It is also evident from the theoretical models, such as given by Rino (1979) and Carrano et al., (2019). In 2019, Acharya and Majumdar found that the samples separated for quiet and disturbed geomagnetic conditions do not significantly vary in their probability density distribution features.

The methodology to calculate ROTI is the same among all studies. However, the GNSS receiver data's sampling rate and the time interval over which a value of ROTI is calculated varies from study to study. The time interval for which ROTI is calculated is a factor that must be taken into account whenever ROTI is compared or checked to indicate the scale size of irregularities (Jacobsen, 2014). The choice of the time interval is generally accepted as 5 min, which is a standard time interval by definition from Pi et al. (1997) that compromises between time resolution and the quality of the ROTI value. Krankowski et al. (2006) used 30 min time interval to calculate ROTI, and the reason stated to use 30 min is to capture the size of

400–1000 km of irregularity size and the speed of the patch structure of 600–800 m/s, the duration of TEC recognized patch is within 15–30 min. Carrano et al. (2019) developed a theoretical relation between ROTI and S4. In this study, an attempt has been made to evaluate the correlation of ROTI and S4 with different averaging intervals to calculate the ROTI, i.e., 3 min, 5 min, and 10 min, and their dependence on various factors. To further investigate the correlation of ROTI and S4 a detailed statistical analysis has been performed.

In the present study, as from the literature survey, it is found that the correlation between ROTI and S4 is not regular. The primary objective is to evaluate the feasibility of using ROTI as a proxy for S4 in the Indian region, which will help use standard GNSS receivers for ionospheric studies. Yang and Liu (2016b) demonstrated that ROTI and S4 correlate well when strong scintillations were considered. In this present work, both strong and weak scintillations are considered.

In the current study, the dependence of the correlation between ROTI and S4 on different factors such as elevation angle, geographic locations, and solar flux (F10.7) was studied in the Indian region. Earlier studies in different geographic sectors have shown that ROTI and S4, are related (Basu et al., 1999; Pi et al., 2013). The Indian region is mainly composed of equatorial and low latitude ionospheric regions, which are more prone to ionospheric irregularities than regions at higher latitudes. The present work primarily focuses on quantifying ROTI in terms of the magnitude of ionospheric scintillation (compared to S4) rather than just an indicator for the presence of scintillation. As most standard receivers do not have a high sampling rate, as discussed above, this study will enable ROTI to be used as a proxy for S4. In this study, the variation of integration time and elevation angle threshold on the ROTI/S4 ratio were investigated to capture the broader aspect of the correlation and variation of ROTI/S4.

2. Data and methodology

In this study, ionospheric scintillation (S4) data and TEC data were collected from Ionospheric Scintillation Monitoring (ISM) - GPS receivers installed at the 25 stations shown in Fig. 1. These special GPS receiver stations were established under the GPS Aided Geo Augmented Navigation (GAGAN) program in collaboration with the Airport Authority of India (AAI). The model of these ISM receivers is Novatel 4004 (Van Dierendonck et al., 1996; Rama Rao et al., 2006a, 2006b; Acharya et al., 2007) and the type of antenna used is the choke ring antenna. The S4 data sampling interval is 1 min, and the TEC data sampling interval is 30 sec that is recorded by the same ISM receiver. The data for years 2014 to 2016, which includes solar activity maximum (the year 2014) of solar cycle 24 and the descending years 2015 and 2016, are used in this study. The following stations, Trivandrum and Port Blair (near-equatorial), Hyderabad (low latitude region), Mumbai and Kolkata (equatorial ionization anomaly region), and Delhi & Jodhpur (beyond ionization anomaly region), are chosen in this present study. These stations selected for the study cover all three geomagnetic latitude zones, viz. equatorial, low latitude, and equatorial ionization anomaly (EIA) regions of the ionosphere in the Indian region.

The scintillation index S4 used in this study is given in equation (1), which is defined as the normalized variance of the intensity of the signal (Yeh & Liu, 1982).

$$S4 = \sqrt{\frac{< I^2 > - < I >^2}{< I >^2}} \tag{1}$$

This S4 index measures the severity of amplitude scintillations caused by trans-ionospheric signals. This index measures rapid variations in the amplitude of radio wave signals caused by small-scale structures of ionospheric irregularities in the ionosphere. The GPS ISM receivers directly calculate the S4 index from the raw data sampled at a 50-Hz as given by equation (1) which is implemented in the receiver firmware (Van Dierendonck et al., 1996; Rama Rao et al., 2006a). Severe scintillation conditions can prevent a GPS receiver from locking on to the received signal and can severely reduce the accuracy of position estimates. Thus, scintillation conditions can reduce the accuracy of positioning results.

ROTI is defined as the standard deviation of the rate of change of TEC, which was estimated from TEC derived from 30 s dual frequency GPS data and averaged over a 5 min period by Pi et al. (1997) as given by equation (2). The rate of change of TEC for the time interval of 1 min is abbreviated as ROT (TECU/min).

$$ROTI = \sqrt{< ROT^2 > - < ROT >^2} \tag{2}$$

We have also estimated ROTI from 30-second dual-frequency (L band) GPS TEC data averaged over 3 min, 5 min, and 10 min time periods as discussed in the later sections.

For the current studies, two types of S4 data sets are considered. (1) S4 values measured from each of the PRNs representing values at each of the ionospheric pierce point (IPP) of that PRN and (2) diurnal S4 values derived from the signals along the ray paths to all PRNs to represent the station where the GPS receiver is installed.

2.1. Derivation of diurnal S4 and diurnal ROTI

For the seasonal and statistical studies of scintillations, a characteristic or diurnal variation of S4 of the particular location is needed. So, the S4 values at ionospheric pierce point locations (IPPs) from different GPS satellites, which are simultaneously visible for a few hours of the day, had to be collectively combined to represent a continuous 24-hour variation. For this, the maximum S4 value from multiple S4 values recorded along the ray paths from different satellites at the same epoch was chosen to represent the

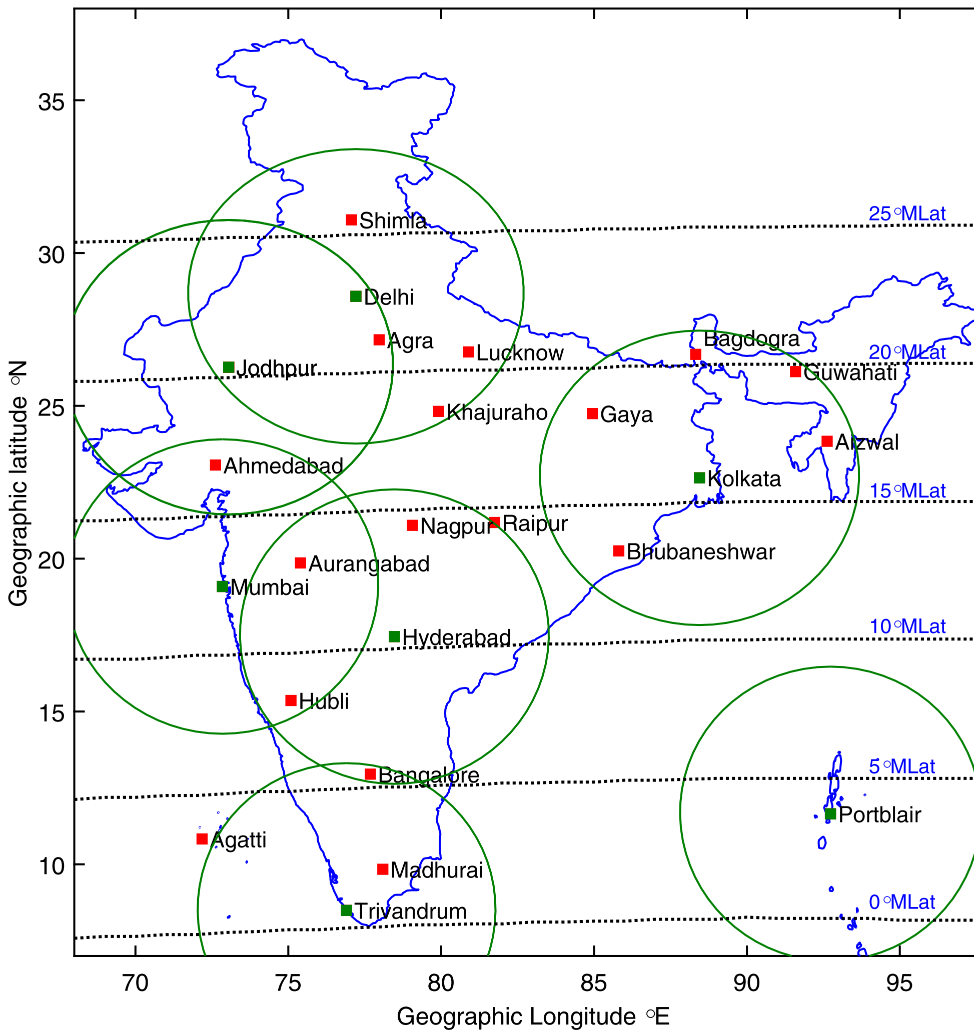

Fig. 1. The locations of the GPS receiver stations in the Indian region. The GPS receivers are indicated by square-filled boxes with station names next to them. The stations marked with green squares have been used in the study. The horizontal dotted lines indicate the magnetic dip latitudes (MLat) with respective values to the right of the figure. The magnetic dip latitudes are calculated using IGRF model with year 2015 coefficients at 350 km ionospheric height. The green circles depict the region covered at 350 km height by selected stations for elevation mask angle of 30 degrees. The crest of EIA lies about at 15 +/- 5 degrees magnetic dip latitudes, which varies with season and solar activity. (For interpretation of the references to color in this figure legend, the reader is referred to the web version of this article.)

worst possible scenario or the maximum ionospheric scintillation encountered by the GPS receiver at that instant.

Fig. 2 shows the diurnal variation of the S4 index derived for all PRNs marked on the y-axis (using an offset for S4 with each PRN) for a typical scintillation day of 31 March 2014, at the station Mumbai. The top panel of Fig. 2 shows the S4 indices for each PRN-wise in blue, and the S4 outlier values as discussed below are indicated in red. From this figure, we can observe noise and multipath induced S4 values at lower elevation angles (at the onset and end of each satellite S4 values) even after an elevation mask of 30 degrees was applied. Such multipath related noisy S4 is particularly evident at 03:00 UT (08:30 local time), when ionospheric scintillations at L-band frequencies are usually absent. Thus to clean the outliers in the data, a systematic approach is followed, as discussed in the following steps.

It is observed that the data contains a considerable amount of noise at lower elevation angles. This noise is attributed to tropospheric scatter and due to multipath (Williams and Neivinski, 2017). This noise has to be removed to observe actual data points that represent scintillations during post-sunset hours. For ionospheric studies using satellite data, the elevation mask is always used by many researchers to reduce the non-ionospheric interferences or spurious scintillations due to multipath signals coming from the horizon (Yang and Liu 2016b, Hernandez-Pajares et al., 2006; Rose et al., 2011). In the present study, the elevation mask angle of 30 degrees was considered to reduce the multipath effects. After applying the elevation mask to the observed data, attempts were made to remove outliers in S4 data due to other noise sources. The outliers are defined as elements that are more than two local scaled Median Absolute Deviation (MAD)

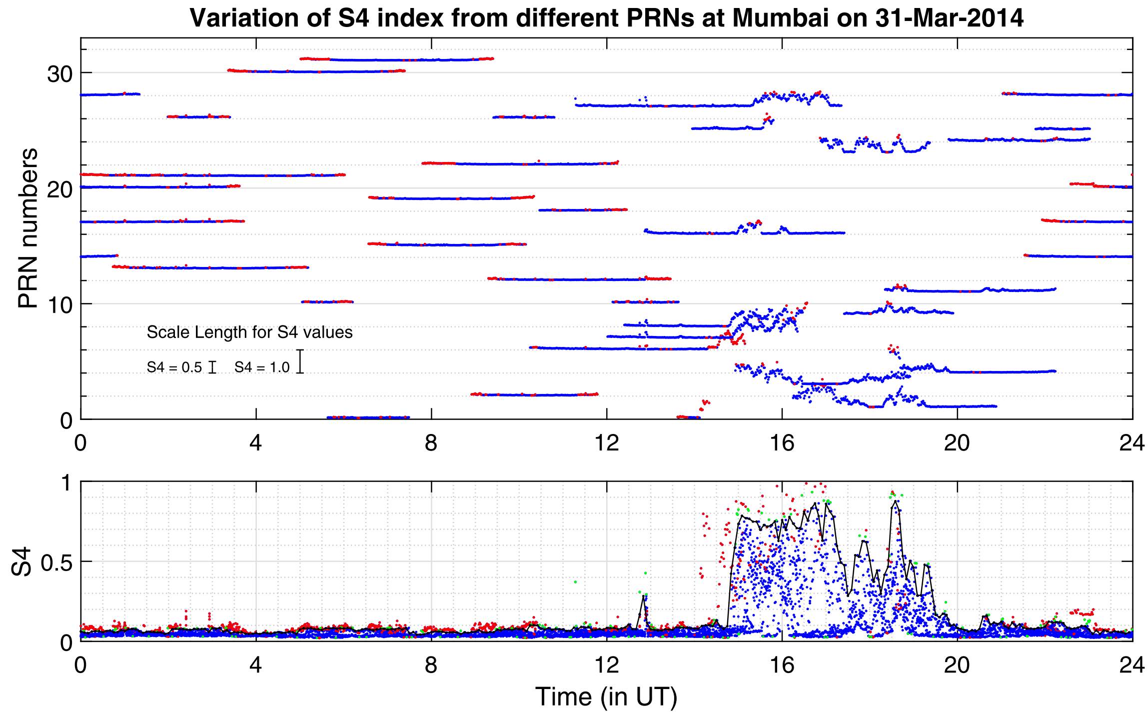

Fig. 2. Noise removal from S4 from individual PRNs and collectively for diurnal variation at station Mumbai for 31 March 2014. In the top panel the y-axis indicates PRN Numbers (constant values), and the S4 is represented with an offset by PRN number. The blue points represent S4 values that are considered for data analysis, the red points are outliers that are omitted and the green points are outliers removed from the populated data points from all PRNs. The diurnal S4 values are plotted in a solid black line in the lower panel, along with S4 values from all PRNs (that are shown individually in top panel). (For interpretation of the references to color in this figure legend, the reader is referred to the web version of this article.)

(Leys et al., 2013) from the local median over a specified window length given by the Eq. (3) and also those values that fall beyond the set percentile threshold values as given in the Table 1.

$$y_i = \begin{cases} x_i, |x_i - \mu| < 2\sigma \\ outlier, |x_i - \mu| \geq 2\sigma \end{cases} \quad (3)$$

where x_i is the data sequence that belongs to fixed window length (see Table 1), the μ is local mean of the selected window length, and σ is its local standard deviation. When the difference between the value x_i and the local mean is greater than two times the local standard deviation, and also it falls beyond set percentile limits given in the Table 1 then it is considered as an outlier.

During the local day time, the outliers that are beyond threshold levels (<1 or > 90 percentile) in each of one-hour bins are marked as outliers in red points for each of the PRN in Fig. 2. As observed from decades of studies, the ionospheric scintillations at L-band frequencies are least expected during the local daytime (Rama Rao et al., 2006a). Likewise, for the night-time period, the S4 values for 12:30 to 23:00 UT (18:00 to 04:30 LT) the outliers that fall beyond percentile thresholds (<1 or > 97 percentile) are removed. This will ensure that any significant S4 value other than random spikes are retained to represent ionospheric scintillation and not removed inadvertently.

In the lower panel of Fig. 2, the S4 values from all the PRNs were populated with corresponding time on the x-axis. Now, outliers that fall beyond threshold percentiles (<1 or >98 percentile) from all the data points collectively from all PRNs binned at 30-minute intervals, were eliminated and indicated by green color. This process is done to remove any outliers whose value is very high or low, compared to the rest of the group in the bin.

From the resultant S4 values, the diurnal S4 variation for the receiver's location was chosen as the series of maximum values among every 5-minute averaging interval from 0 to 24 h. These values would represent the worst possible scenario or the maximum ionospheric scintillation

Table 1
Window lengths for MAD and percentile limits for outlier detection.

Time (UT)	Window length for MAD	Percentile limits	Outlier color
For individual PRNs – as shown in top panel of Fig. 2			
00:00 to 12:30 UT	1 h	< 1, > 90	red
12:30 to 23:00 UT	1 h	< 1, > 97	red
For data from all PRNs – as shown in bottom panel of Fig. 2			
00:00 to 24:00 UT	30 min.	< 1, > 98	green

encountered by the GPS receiver at that instant. This method is validated manually by checking the resultant S4 data set from a couple of selected stations and for chosen scintillation dates to check for any unwanted removal of data or any artificial induced ionospheric scintillation signatures. From here on, the terms mentioned in this paper, "diurnal S4" and "diurnal ROTI," means the maxima of the values binned at 5-minute intervals from multiple PRNs present in those time bins, as described in this section.

Fig. 3 shows the diurnal variation of S4 for one year with days on the x-axis and time on the y-axis for the station Mumbai. The color scale on the right-hand side gives S4 values color-coded in the figure. This figure is drawn using the diurnal S4 following the above-discussed procedure. This figure clearly shows the diurnal variation of each of the days and collectively shows the seasonal occurrence pattern of S4, which is well in agreement with previous studies. Also, selected cases have been carefully examined to validate diurnal S4 values and compared with S4 values from each of the satellites. And it is noticed that they match very well, representing the scintillation durations and intensities. From Fig. 3, the multipath is seen as diagonal pattern of low S4 values, their slope is nearly 4 min per day as the GPS satellite orbital period is exactly half a sidereal day. The multipath S4 values are below 0.1 that is considered as noise. This confirms that outlier removal was used carefully to eliminate noise but not scintillation data due to the ionospheric origin, and most of the scintillation data has been captured in the diurnal S4.

Similarly, after calculating ROTI from 5-min ROT values (Pi et al., 1997), the spikes and noisy data were removed as discussed in the above section of outlier and noise removal. Similarly, diurnal ROTI is calculated as a series of maximum values among every 5-min interval bin from 00:00 to 24:00 UT. Fig. 4 shows diurnal S4, and diurnal ROTI values. The Fig. 4 depicts that both the onset and duration of ROTI correspond well with that of the S4 index, but the magnitudes do not correspond as documented in earlier studies (Basu et al., 1999). Hence in this study, attempts are made to estimate S4 values from the derived ROTI.

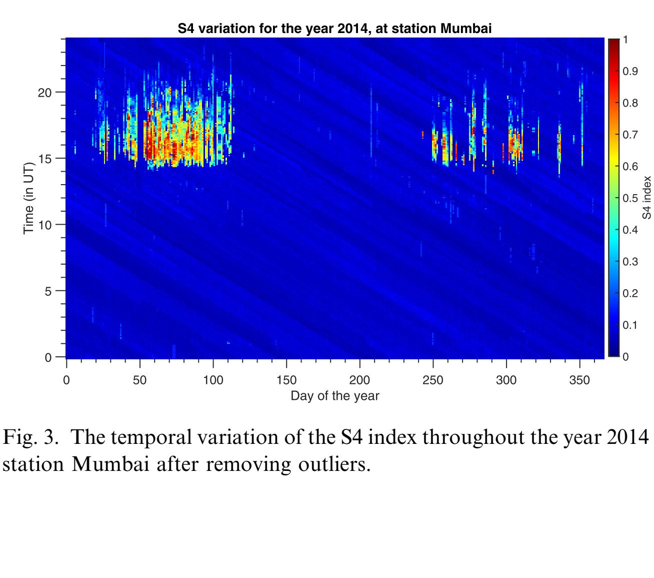

Fig. 3. The temporal variation of the S4 index throughout the year 2014 at station Mumbai after removing outliers.

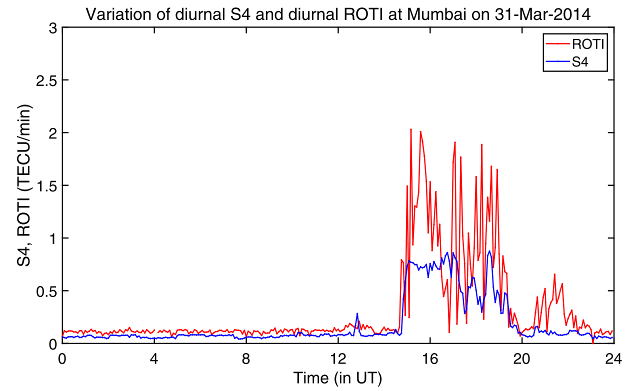

Fig. 4. Diurnal variations of ROTI and S4 for 31 March 2014 after noise removal, at Mumbai station.

3. Results and discussion

As it is evident from the definition of S4, a special Ionospheric Scintillation Monitoring - GPS receiver is required to record the S4 index, as it is derived from the high rate amplitude of the received signal. Thus, the regular dual GNSS frequency that most commonly records the pseudorange and phase observables at 30 s or 1-second sampling interval cannot be used to derive the S4 index. The S4 index is a helpful parameter to check whether the received signal is subjected to ionospheric scintillation or not. Many research studies have been carried out to derive similar index from TEC data which can be a proxy to the S4 index. ROTI is the most frequently used alternate parameter to the S4 index (Li et al., 2020). One can check the presence of ionospheric scintillation from the ROTI value but cannot estimate the exact magnitude of ionospheric scintillation index S4. Many studies done so far have given the range of ratios of S4 to ROTI values, but those ratios were found to be varying geographically (Basu et al., 1999). Hence in this study, the S4 and ROTI values were studied, employing correlation and statistical methods to see how they relate in the Indian ionospheric regions.

The correlation between the indices, S4 and ROTI, was analyzed from seven stations for three years individually from 2014 to 2016 to understand the relation between them. Also, ROTI is calculated for three averaging periods. The findings obtained from this study will enable us to take advantage of the large amount of GPS data recorded by standard GPS receivers to study ionospheric scintillations using ROTI as a proxy for S4.

Fig. 5 shows the correlation between diurnal ROTI and diurnal S4 values (a, b, c), and also the correlation between ROTI and S4 values (d, e, f) for different elevation-mask angles of 30, 50, and 70 degrees, respectively. In this figure, the data from the Mumbai station for the year 2014 is shown. For this correlation analysis, the data was chosen from scintillation days and for the duration of scintillation

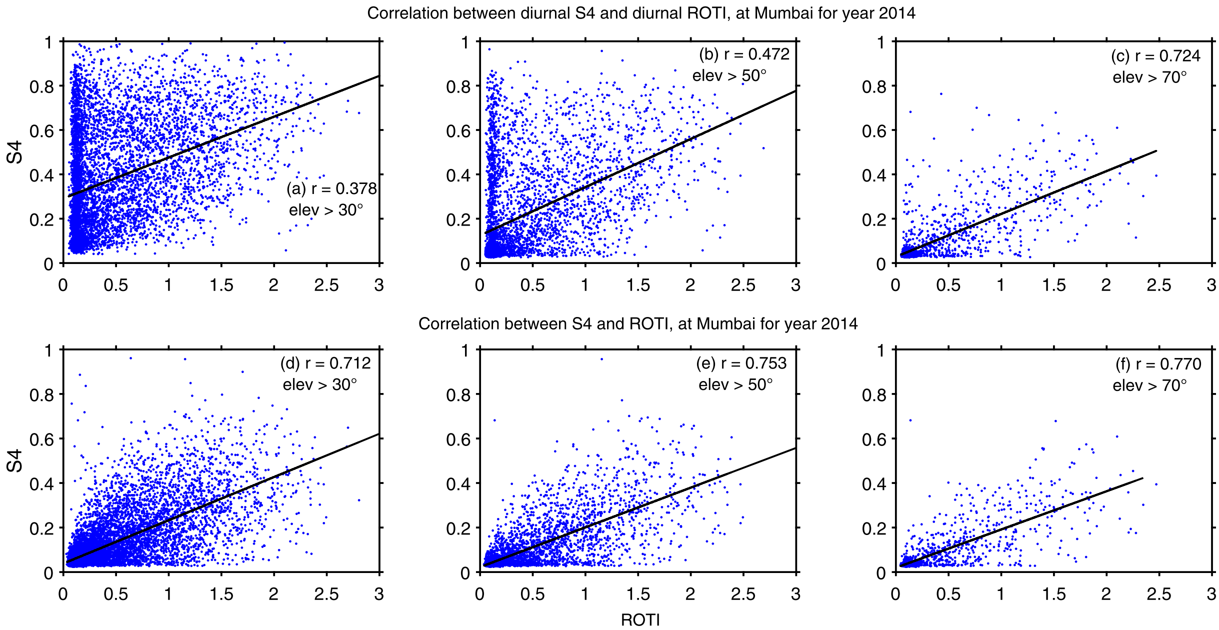

Fig. 5. Correlation between diurnal S4 and diurnal ROTI (figures a, b, and c), correlation between S4, and ROTI values (figures d, e, and f) for different elevation angles greater than 30, 50, and 70 degrees, respectively.

identified from the S4 index. The scintillation days are marked when the S4 values are greater than 0.2 for at least 5 min. Many studies have categorized S4 values of 0.2 as weak scintillations (Bhattacharyya et al., 2017). In the present study, also S4 greater than 0.2 is considered. An additional 5 min of data before and after the event time is added to the scintillation patch to capture the evolution and include how ROTI varies with S4 values less than 0.2. These conditions are used for selecting data from both diurnal and regular (individually from all PRNs) values of S4 and ROTI.

As we can see from Fig. 5, the ROTI and S4 values (d, e, and f) correspond to each other (from correlation ratio) better than the diurnal ROTI and diurnal S4 (a, b, and c). This is expected as both the values S4 and ROTI reflect the data observed from the same PRN. And in the case of diurnal S4 and diurnal ROTI, they represent values of the station, selected as the maxima of data points from all PRNs in that time bin observed. Therefore, in that time bin, which also includes spatial data from different satellites, the maxima values of diurnal S4 and diurnal ROTI may not be from the same PRN. Thus, the correlation between diurnal S4 and ROTI is relatively less than S4 and ROTI, and the correlation values improve with increasing elevation angle.

From Fig. 5(a, b), we can see that there are many values of diurnal S4 corresponding to lower values of diurnal ROTI. This is expected as the ROTI value is calculated for every 5 min, resulting in few values, i.e., one value in each 5 min time bin. But in the S4 dataset, there will be many values in each of the 5-min time bin (for each PRN). The maximum S4 value (diurnal S4) is chosen from that 5-min time bin from all the PRNs. Also, scintillation may not be equally present in all the PRNs due to spatial variations. So we see a wide variation of diurnal S4 values corresponding to low values of diurnal ROTI. As the elevation angle is increased, the data is limited and converged to the station's overhead, and the spatial variation is reduced. Thus, both diurnal S4 and diurnal ROTI correspond better with higher elevation, as shown in Fig. 5(c). We can see that the diurnal values (diurnal S4, diurnal ROTI) can represent the onset effect of ionospheric scintillation and its duration at that station from Fig. 4. Due to the poor correlation between diurnal ROTI and diurnal S4, we use S4 and ROTI for further analysis.

Many researchers have also studied ROTI with different averaging intervals to capture different scale sizes of irregularities, obviously much larger than the Fresnel zone size (at L-band frequency) as the sampling interval is larger. Therefore, in this study, ROTI of two other averaging intervals, 3 min, and 10 min, along with standard 5-min ROTI were also calculated to see how they correlate with the S4 index in the Indian region. Fig. 6 shows the correlation between S4 and ROTI values from different averaging intervals, for elevation angles from 30 to 70 degrees, for three years 2014, 2015, and 2016.

From Fig. 6, we can see that for equatorial and low latitude stations, there is some increase in correlation with increasing elevation angle for the year 2014. Otherwise, for other years 2015 and 2016, the correlation increases up to 50 degrees elevation, and afterward, it decreases for many stations. Also, the solar activity is in declining phase during the years 2015 (mean sunspot no. 69.80) and 2016 (mean sunspot no. 39.80), which is less active compared to the year 2014 (mean sunspot no. 113.30), resulting in less ionospheric scintillation occurrence rate (Rama Rao et al., 2006a) as well as lower TEC values. With higher elevation angles, the number of data points will be less. For example

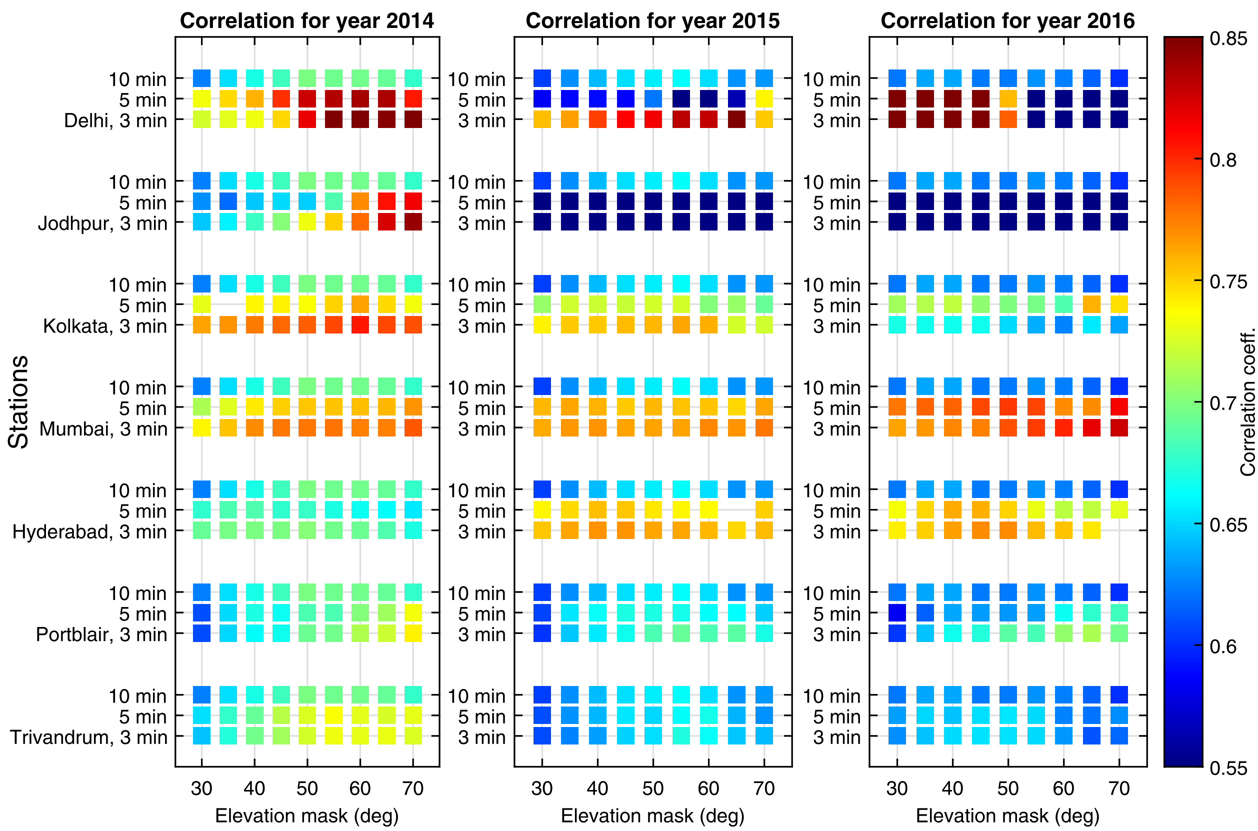

Fig. 6. The elevation dependence of correlation between ROTI and S4 for years 2014–2016, and also using different averaging time intervals for ROTI calculation, i.e., 3 min, 5 min, and 10 min indicated on y-axis, for seven chosen stations. The increased elevation mask angle from 30 to 70 degrees is shown on the x-axis. The correlation coefficient is color-coded (filled square boxes) as per the color bar on the right-hand side.

from Delhi, the scintillations observed will be mostly in south direction and away from zenith as this station's location is north of EIA region. As elevation mask angle increases, the lower elevation data points are removed which may contain scintillation particularly if those contain scintillation observations at locations far away from zenith. Thus increased elevation mask at times may progressively eliminate the visible regions where scintillations occur. Thus at Delhi, the correlation at higher elevation angles might have become less for the years 2015 and 2016. This could be the reason why the correlation between S4 and ROTI is not systematic with increasing elevation angle in all the cases. The correlation between 10-min ROTI and S4 is lower than for the other two ROTI averaging intervals and is not proportional to elevation angle in most cases. The correlation values of 3-min ROTI vs. S4 are marginally high at few instances when compared to 5-min ROTI and 10-min ROTI cases. The reason could be the size of irregularities detected by ROTI, which are the order of a few km, and becomes larger as we increase the time interval and does not correlate well with small size (∼360 m) irregularities detected by S4 at GPS L1 frequency. So, to use ROTI as a proxy for S4, it is observed from this study that the time duration over which averaging is done plays a significant role depending on the size of irregularities detected by S4. Hence, ROTI calculated from a 5 min interval is good enough as a proxy for S4 in the Indian region.

Thus, except for the year 2014 and at equatorial & low latitude regions, the correlation between S4 and ROTI (all three averaging intervals 3, 5, and 10 mins) do not have a proportional increase with elevation angle. There is no strict increase in correlation coefficient with increasing elevation mask angles, as shown in Fig. 6 for EIA and beyond EIA regions for years 2015 and 2016. This could be attributed to the reduced number of data points, or spatial coverage of scintillation affected areas is reduced/eliminated due to elevation mask angle. From this exercise, it can be observed that the elevation threshold does not play a significant role in affecting the correlation between S4 and ROTI values. The 3-min interval ROTI values have a marginally high correlation with S4 compared to 5-min ROTI. Hence, in the rest of the results, only 5-min standard ROTI is considered. A similar exercise was carried out to see if the correlation coefficient between S4 and ROTI varies with F10.7 values for the data of 3 years 2014–2016, but not no conclusive proportionality is found.

From Fig. 5 (d, e, and f), statistically, ROTI and S4 correlate well. To reduce observation bias due to the density of data points, binning is done using a step size of 0.1 for ROTI and a step size of 0.05 for S4. These binned values are scaled with a total number of data points present in the ROTI columns with the same bin value. These scaled values are shown in Fig. 7, in percentages of that bin with respect to total data points across all S4 bins to the corresponding ROTI value. For example, in Fig. 7, each value S4 bin for the given ROTI (say ROTI bin = 0.5 to 0.55) is the percentage of data points in that bin to the total number of all data points in all S4 data bins (for all S4 values from 0 to 1.0) that correspond to that ROTI bin (of 0.5 to 0.55).

The Fig. 7 (a, b, and c) shows the percentage occurrence of diurnal S4 value to corresponding diurnal ROTI value, and the Fig. 7 (d, e, and f) show percentage occurrence of S4 to corresponding ROTI values for the respective stations Trivandrum (equatorial region), Hyderabad (low latitude region), and Kolkata (EIA region). As can be seen from Fig. 7 (top panel), except at the equatorial station Trivandrum, the percentage of diurnal S4 values varies in a wide range that corresponds to each of the diurnal ROTI bin value, in comparison to S4 vs. ROTI (figures on bottom panels). At equatorial stations, irregularities scale sizes are larger than low latitude and EIA regions (Wernik et al., 2003), and ROTI represents large scale irregularities, which could be one reason why diurnal S4 and ROTI values correspond better (relative to other stations) at this equatorial station Trivandrum.

We can observe from Figs. 5 and 7 that ROTI and S4 values correspond better than the diurnal values, which is expected, as they are determined along the ray paths from the same PRN to the same receiver location. Therefore, to estimate the probable S4 value from the calculated ROTI, the percentage occurrence from Fig. 7 (d, e, and f) are used.

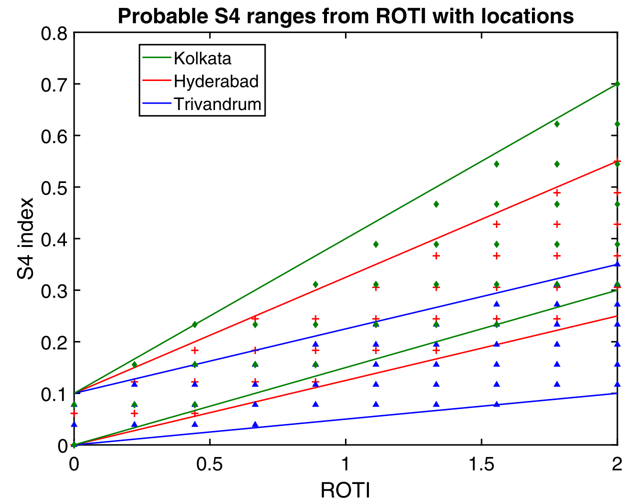

Fig. 8. The figure shows the most probable S4 ranges corresponding to ROTI values at different locations viz Trivandrum (equatorial region), Hyderabad (low latitude region), Kolkata (EIA region) indicated by blue, red, and green lines (for both upper and lower bounds) respectively. The area between respective lower & upper boundary lines is filled with symbols of triangles, plus signs, and diamonds of the same colors, respectively. (For interpretation of the references to color in this figure legend, the reader is referred to the web version of this article.)

Even though the correlation is in the range of 0.6 to 0.8 for the considered stations (see Fig. 6), there is a spread of data points, and one will not be able to use a linear

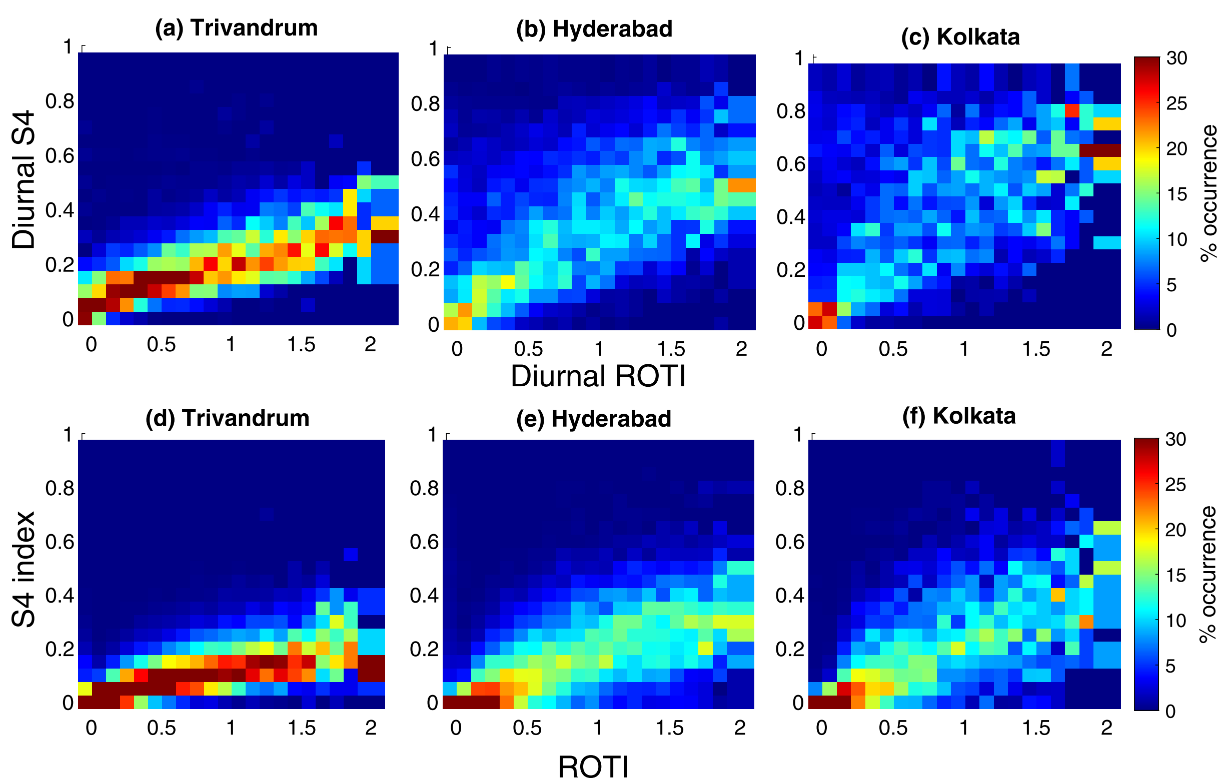

Fig. 7. The top panel (a, b and c) shows the percentage occurrence of diurnal S4 value to corresponding diurnal ROTI value for the stations Trivandrum (equatorial region), Hyderabad (low latitude region), and Kolkata (EIA region). The bottom panel (d, e, and f) shows the percentage occurrence of S4 value to the corresponding ROTI value for the same respective stations. The color bar indicates the color code of the percentage occurrence of S4.

Table 2
The probable range of S4 at corresponding regions for a given ROTI value.

ROTI value	Equatorial region, S4 values	Low-latitude region, S4 values	EIA region, S4 values
0	0–0.1	0–0.1	0–0.1
0.5	0–0.2	0.05–0.25	0.05–0.3
1.0	0.05–0.25	0.1–0.35	0.15–0.4
1.5	0.1–0.3	0.15–0.4	0.25–0.55
2.0	0.1–0.35	0.25–0.55	0.3–0.7

equation to estimate S4 from ROTI with reasonable accuracy. It is observed from Fig. 7(d, e, and f) that a range of S4 values with up to 80% probability corresponds to a single calculated ROTI value. Fig. 8 shows the lower and upper bounds of the S4 values range for each of the ROTI bin for three different stations as considered in Fig. 7. These lines are drawn in Fig. 8, indicating the ranges chosen so that at least 80% of the S4 data points fall within the station's respective upper & lower ranges. The upper and lower range of S4 values obtained from Fig. 8 and shown in Fig. 7 are tabulated in Table 2.

Thus for a given ROTI value from the region (equatorial, low latitude, and EIA region) will have a corresponding S4 value within the given range, as shown in Table 2. As observed from Fig. 7 (d, e, f) and 8, and Table 2, this range of S4 values corresponding to ROTI value systematically increases with geographic latitudes from equatorial to EIA region in the present study of the Indian ionospheric region.

4. Summary

The present study focuses on the possibility of estimating the S4 index from the ROTI value that is calculated from TEC. As known from earlier studies (Basu et al., 1999), the S4 index is a good measure of ionospheric scintillation that affects the L-band signals (in GNSS receivers).

For calculating the S4 index, a high sampling (50 Hz) of the signal-to-noise ratio is needed (Yang & Liu, 2016a). Only special GNSS receivers, i.e., ionospheric scintillation monitors with high sampling rates, are specifically meant for these ionospheric scintillation studies. The dual-frequency GNSS receivers that are very popularly used for various studies, in general, have a lower sampling interval of 30 s. ROTI at 5-minute intervals can be calculated from these receivers that are widely used. ROTI values are also calculated for intervals of 3 mins and 10 mins, apart from 5 mins to study the correlation with S4 values. It is found out that 10-min ROTI values did not have a good correlation with S4. Also, 3-min ROTI had a marginal increase (of about 0.05) correlation with S4 at low latitude region, compared to ROTI and S4. Therefore, changing the standard interval (5 min) for ROTI calculation is not effective in the Indian region. It is observed that diurnal ROTI and diurnal S4 are suitable to study the specific station temporally and not useful in correlating ROTI with S4, as they take only maximum effect from all the values ignoring spatial variation.

The correlation between ROTI and S4 had been studied by several researchers, and results indicate that the correlation and ratio changes with geographic location. From the present study, the correlation between S4 and ROTI is in the range of 0.6 to 0.8. And the median ratio of ROTI to S4 values are of the order of 10, 5, and 4 respectively at equatorial, low latitude, and EIA regions, respectively. It is observed from Fig. 8 and Table 2 that the ROTI/S4-ratio systematically decreases from the equatorial region to EIA region latitudes.

An exact value of S4 cannot be estimated from the ROTI value, as the ROTI usually responds to the irregularity of large scale sizes, whereas the S4 index is caused by Fresnel zone scale irregularities that are orders of magnitude smaller than those detected by ROTI. Thus, from the present study, the most probable range of S4 value is estimated from the ROTI value as given in Table 2.

Declaration of Competing Interest

The authors declare that they have no known competing financial interests or personal relationships that could have appeared to influence the work reported in this paper.

Acknowledgements

This work is supported by the Indian Institute of Geomagnetism (IIG), Department of Science and Technology, India. The authors thankfully acknowledge Space Application Center (SAC), ISRO Ahmedabad, for providing GPS data from the GAGAN network repository. The GAGAN Data is available through Acharya and Majumdar (2019). The sunspot number data has been obtained from WDC-SILSO, Royal Observatory of Belgium, Brussels (http://sidc.be/silso/). One of the authors (C.K.) is grateful to IIG for the fellowship awarded towards her Ph.D. One of the authors (D.J.S.) acknowledges the support of SAC, ISRO for ISRO-respond project grant no: ISRO/RES/4/631/2016-17.

References

Abadi, P., Otsuka, Y., Tsugawa, T., 2015. Effects of pre-reversal enhancement of E x B drift on the latitudinal extension of plasma bubble in Southeast Asia. Earth, Planets and Space (2015) 67:74 DOI 10.1186/s40623-015-0246-7.

Acharya, R., Majumdar, S., 2019. Statistical relation of scintillation index S4 with ionospheric irregularity index ROTI over Indian equatorial region. Adv. Space Res. 64 (5), 1019–1033. https://doi.org/10.1016/j.asr.2019.05.018.

Acharya, R., Nagori, N., Jain, N., Sunda, S., Regar, S., Sivaraman, M.R., Bandopadhyay, K., 2007). Ionospheric Studies for the implementation of GAGAN. Indian Journal of Radio Space Physics, Vol. 36, pp. 394-404, October, 2007.

Basu, S., Basu, S.u., Aarons, J., McClure, J.P., Cousins, M.D., 1978. On the coexistence of kilometer- and meter-scale irregularities in the nighttime equatorial F region. J. Geophys. Res. 83 (A9), 4219–4226. https://doi.org/10.1029/JA083iA09p04219.

Basu, S., Groves, K. M., Quinn, J.M., & Doherty P. (1999). A comparison of TEC fluctuations and scintillations at Ascension Island. Journal of Atmospheric and Solar-Terrestrial Physics, 61(16), 1219-1226. https://doi.org/10.1016/S1364-6826(99)00052-8.

Carrano, C.S., Groves, K.M., Rino, C.L., 2019. On the relationship between the rate of change of total electron content index (ROTI), irregularity strength (CkL), and the scintillation index (S4). J. Geophys. Res. Space Phys. 124, 2099–2112. https://doi.org/10.1029/2018JA026353.

Beach, T.L., Kintner, P.M., 1999. Simultaneous Global Positioning System observations of equatorial scintillations and Total Electron Content fluctuations. J. Geophys. Res. 104 (A10), 22553–22565.

Bhattacharyya, A., Kakad, B., Gurram, P., Sripathi, S., Sunda, S., 2017. Development of intermediate-scale structure at different altitudes within an equatorial plasma bubble: Implications for L-band scintillations. J. Geophys. Res. Space Phys. 122 (1), 1015–1030. https://doi.org/10.1002/2016JA023478.

Farley, D.T., Balsey, B.B., Woodman, R.F., 1970. Equatorial spread F: Implications of VHF radar observations. J. Geophys. Res. Space Phys. 75 (34), 7199–7216. https://doi.org/10.1029/JA075i034p07199.

Fejer, B.G., 1997. The electrodynamics of the low latitude ionosphere: recent results and future challenges. J. Atmos. Sol. Terr. Phys. 59 (13), 1456–1482. https://doi.org/10.1016/S1364-6826(96)00149-6.

Hernandez-Pajares, M., Juan, J.M., Sanz, J., 2006. Medium-scale traveling ionospheric disturbances affecting GPS measurements: spatial and temporal analysis. J. Geophys. Res. 111, A07S11. https://doi.org/10.1029/2005JA011474.

Huang, C.S., Kelley, M.C., 1996. Nonlinear evolution of equatorial spread F: On the role of plasma instabilities and spatial resonance associated with gravity wave seeding. J. Geophys. Res. Space Phys. 101 (A1), 283–292. https://doi.org/10.1029/95JA02211.

Hysell, D.L., 2000. An overview and synthesis of plasma irregularities in equatorial spread F. J. Atmos. Sol. Terr. Phys. 62 (12), 1037–1056. https://doi.org/10.1016/S1364-6826(00)00095-X.

Jacobsen, K.S., 2014. The impact of different sampling rate and calculations time intervals on ROTI values. J. Space Weather Space Climate 4, A33. https://doi.org/10.1051/swsc/2014031.

Kelley, M.C., 1985. Equatorial spread-F: Recent results and outstanding problems. J. Atmos. Terrest. Phys. 47(8-10), 745-752. https://doi.org/10.1016/0021-9169(85)90051-0.

Kelley, M.C., 1989. The Earth's ionosphere, Plasma Physics and Electrodynamics. Academic Press, San Diego, CA.

Klobuchar, J.A., Iyer, K.N., Vats, H.O., Rastogi, R.G., 1977. A numerical model of equatorial and low latitude total electron con-tent for use by satellite tracking systems for ionospheric corrections. Indian J. Radio Space Phys. 6, 159–164 http://nopr.niscair.res.in/handle/123456789/37436.

Kintner, P.M., Ledvina, B.M., de Paula, E.R., 2007. GPS and ionospheric scintillations. Space Weather 5 (9), S09003. https://doi.org/10.1029/2006SW000260.

Krankowski, A., Shagimuratova, I.I., Baran, L.W., Ephishov, I.I., Tepenitzyna, N.J., 2006. The occurrence of polar cap patches in TEC fluctuations, detected using GPS measurements in southern hemisphere. Adv. Space Res. 38 (11), 2601–2609. https://doi.org/10.1016/j.asr.2005.12.006.

Leys, C., et al., 2013. Detecting outliers: Do not use standard deviation around the mean, use absolute deviation around the median. J. Exp. Soc. Psychol. (2013), http://dx.doi.org/10.1016/j.jesp.2013.03.013.

Li, Q., Zhu, Y., Fang, K., Fang, J., 2020. Statistical Study of the Seasonal Variations in TEC Depletion and the ROTI during 2013–2019 over Hong –Kong. Sensors (MDPI) 67 (1). https://doi.org/10.3390/s20216200.

Ma, G., Maruyama, T., 2006. A super bubble detected by dense GPS network at East Asian longitudes. Geophys. Res. Lett. 33 (11), L21103. https://doi.org/10.1029/2006GL027512.

McClure, J.P., Hanson, W.B., Hoffman, J.H., 1977. Plasma bubbles and irregularities in the equatorial ionosphere. J. Geophys. Res. 82 (19), 2650–2656. https://doi.org/10.1029/JA082i019p02650.

Olwendo, J.O., Cilliers, P., Weimin, Z., Ming, O., Yu, X., 2018. Validation of ROTI for ionospheric amplitude scintillation measurements in a low-latitude region over Africa. Radio Sci. 53 (7), 876–887. https://doi.org/10.1029/2017RS006391.

Ossakow, S.L., 1981. Spread-F theories-a review. J. Atmos. Terr. Phys. 43 (5–6), 437–445. https://doi.org/10.1016/0021-9169(81)90107-0.

Otsuka, Y., Ogawa, T., Effendy, 2009. VHF radar observations of nighttime F-region field-aligned irregularities over Kototabang, Indonesia. *Earth Planets and Space 61(4), 431–437. https://doi.org/10.1186/BF03353159*.

Pi, X., Mannucci, A.J., Lindqwister, U.J., Ho, C.M., 1997. Monitoring of global ionospheric irregularities using the Worldwide GPS Network. Geophys. Res. Lett. 24 (18), 2283–2286. https://doi.org/10.1029/97GL02273.

Pi, X., Mannucci, A.J., Spaight, B., Yoaz, B.S., Romans, L.J., Skone, S., Sparks, L., 2013. Observations of global and regional ionospheric irregularities and scintillation using GNSS tracking networks. In: Proceedings of the ION 2013 Pacific PNT Meeting, pp. 752–761.

Rama Rao, P.V.S., Gopi Krishna, S., Niranjan, K., Prasad, D.S.V.V.D., 2006a. Study of spatial and temporal characteristics of L-band scintillations over the Indian low latitude region and their possible effects on GPS navigation. Ann. Geophys. 24 (6), 1567–1580. https://doi.org/10.5194/angeo-24-1567-2006.

Rama Rao, P.V.S., Gopi Krishna, S., Niranjan, K., Prasad, D.S.V.V.D., 2006b. Temporal and spatial variation in TEC using simultaneous measurements from the Indian GPS network of receivers during the low solar activity period of 2004–2005. Ann. Geophys. 24, 3279–3292. https://doi.org/10.5194/angeo-24-3279-2006.

Rino, C.L., 1979. A power law phase screen model for ionospheric scintillation: 1. Weak scatter. Radio Science 14 (6), 1135–1145. https://doi.org/10.1029/RS014i006p01135.

Rose, J.A.R., Tong, J.R., Allain, D.J., Mitchell, C.N., 2011. The use of ionospheric tomography and elevation masks to reduce the overall error in single-frequency GPS timing applications. Adv. Space Res. 47 (2), 276–288. https://doi.org/10.1016/j.asr.2010.05.030.

Tiwari, R., Strangeways, H.J., Tiwari, S., Ahmed, A., 2013. Investigation of ionospheric irregularities and scintillation using TEC at high latitude. Adv. Space Res. 52 (6), 1111–1124. https://doi.org/10.1016/j.asr.2013.06.010.

Van Dierendonck, A.J., Fenton, P., Klobuchar, J., 1996. Commercial ionospheric scintillation monitoring receiver development and test results. Proceedings of the Institute of Navigation's 52nd Annual Technical Meeting.

Wernik, A.W., Secan, J.A., Fremouw, E.J., 2003. Ionospheric irregularities and scintillation. Advances in Space Research, Volume 31, Issue 4, 2003, Pages 971-981, ISSN 0273-1177, https://doi.org/10.1016/S0273-1177(02)00795-0.

Williams, S.D.P., Neivinski, F.G., 2017. Tropospheric delays in ground-based GNSS multipath reflectometry—Experimental evidence from coastal sites. J. Geophys. Rev.: Solid Earth 122 (3), 2310–2327. https://doi.org/10.1002/2016JB013612.

Yang, Z., Liu, Z., 2016a. Observational study of ionospheric irregularities and GPS scintillations associated with the 2012 tropical cyclone Tembin passing Hong Kong. J. Geophys. Res.-Space Phys. 121, 4705–4717. https://doi.org/10.1002/2016JA022398.

Yang, Z., Liu, Z., 2016b. Correlation between ROTI and Ionospheric Scintillation Indices using Hong Kong low-latitude GPS data. GPS Solutions 20 (4), 815–824. https://doi.org/10.1007/s10291-015-0492-y.

Yeh, K.C., Liu, C.H., 1982. Radio wave scintillations in the ionosphere. Proceedings of the IEEE 70(4), 324–360. https://doi.org/10.1109/PROC.1982.12313.